INTRUDER CONFIGURATIONS IN ^{26,28}Ne AND ^{30,32,34}Mg

B.V. Pritychenko, T. Glasmacher, P.D. Cottle[a], M. Fauerbach[a], R.W. Ibbotson, K.W. Kemper[a], V. Maddalena, A. Navin, R. Ronningen, A. Sakharuk, H. Scheit and V.G. Zelevinsky

Nuclear data on masses, level energies and electromagnetic matrix elements in a group of neutron-rich nuclei in the vicinity of ^{32}Mg have indicated the existence of an "island of inversion" in which isotopes at or near the $N = 20$ shell closure have large deformations. The observation of binding energies considerably larger than those expected from conventional shell model calculations provided first evidence for large deformations in this region [1-5]. Further support for the existence of the island of inversion was supplied by the measurement of an anomalously low energy for the 2_1^+ state in the $N = 20$ isotope ^{32}Mg [6] and a large value for the reduced matrix element $B(E2; 0_{gs}^+ \rightarrow 2_1^+)$, which indicated a quadrupole deformation parameter of $\beta_2 \approx 0.5$ [7].

In this report, we present an experimental study of the spectroscopy of the low-lying states in several even-even isotopes of neon and magnesium that are located both in the island of inversion and on its periphery using the technique of intermediate energy Coulomb excitation with radioactive beams. These results include the first measurements of $B(E2; 0_{gs}^+ \rightarrow 2_1^+)$ in ^{26,28}Ne and ^{30}Mg. Our results provide a more complete picture of the extent of the island of inversion and the role of the intruder states outside the boundaries of the island of inversion.

The present experiments were performed at the National Superconducting Cyclotron Laboratory (NSCL) at Michigan State University, and the primary beams for the present experiment were produced with the NSCL superconducting electron resonance ion source and the K1200 superconducting cyclotron. All secondary beams were obtained via fragmentation of the primary beams in a thick ^{9}Be primary target located at the mid-acceptance target position of the A1200 fragment separator [8]. A primary beam of ^{48}Ca^{13+} was used to produce the secondary beams of ^{28}Ne, ^{32}Mg and ^{34}Mg. The secondary beams of ^{26}Ne and ^{30}Mg were made with a primary beam of ^{40}Ar^{12+}.

The γ-ray spectra produced in Coulomb interaction between projectile nuclei and gold target, both without the Doppler correction (so that the spectrum is seen in the laboratory frame) and with the Doppler correction (as seen in the projectile frame) for ^{26,28}Ne and ^{30,32,34}Mg are shown in Fig. 1. Photons deexciting the previously observed 2_1^+ states in ^{30}Mg and ^{32}Mg (at 1482 and 885 keV, respectively) are apparent in the projectile-frame spectra for those two nuclei. A strong peak occurs in the projectile-frame spectrum for ^{26}Ne at 1990(12) keV, while a somewhat weaker (though still clear) peak appears in the corresponding ^{28}Ne spectrum at 1320(20) keV. On the basis of these observations, we propose that the 2_1^+ states occur at these energies in ^{26,28}Ne. The results on the 2_1^+ state energies in the neon isotopes are consistent with those reported at a recent conference [9]. Only a few counts appear in the ^{34}Mg spectrum above a Doppler-shifted energy of 800 keV. Below this energy, there is background due to the Coulomb excitation of the gold target. One other important feature in the ^{32}Mg spectrum is a small second peak in the spectrum at 1438(12) keV, an energy which agrees with a γ-ray observed at 1436(1) keV in the β-decay of ^{32}Na [10,11]. Klotz *et al.* [11] determined that the 1436 keV γ-ray is in coincidence with the 885 keV $2_1^+ \rightarrow 0_{gs}^+$ γ-ray and, therefore, that it deexcites a state at 2321 keV.

For ^{26,28}Ne and ^{30}Mg, where the 2_1^+ states do not appear to be fed by higher-lying states, the cross sections for populating the 2_1^+ states can be determined in a straightforward way. The population cross sections for the 2_1^+ states of these nuclei can then be used to obtain $B(E2; 0_{gs}^+ \rightarrow 2_1^+)$ values using

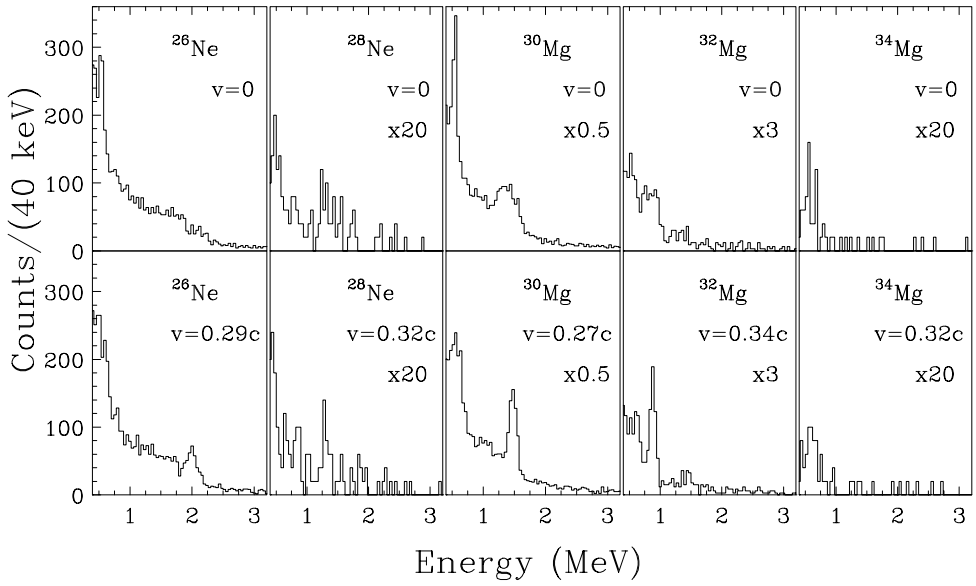

Figure 1: Upper panels contain background subtracted photon spectra in the laboratory frame. The 547 keV $(7/2^+ \rightarrow g.s.)$ transition in the gold target is visible as a peak, while the $(2^+ \rightarrow g.s.)$ transitions in each projectile are very broad. Lower panels contain Doppler-corrected, background-subtracted γ-ray spectra.

Table 1: Experimental parameters and results.

	E_{beam} (MeV/A)	Total beam particles/10^6	$E(2_1^+)$ (keV)	$\sigma(0^+_{g.s.} \rightarrow 2^+)$ (mb)	$B(E2; 0^+_{g.s.} \rightarrow 2^+)$ (e^2fm^4)
^{26}Ne	41.7	39.83	1990(12)	74(13)	228(41)
^{28}Ne	53.0	1.46	1320(20)	68(34)	269(136)
^{30}Mg	36.5	98.35	1481(3)	78(7)	295(26)
^{32}Mg	57.8	6.46	885(9)	80(17)	333(70)
^{34}Mg	50.6	0.22		≤ 164	≤ 670

the formalism of Winther and Alder [12], and these reduced matrix elements are also listed in Table I. In the case of ^{32}Mg, the 2_1^+ state is not only populated directly in the intermediate energy Coulomb excitation reaction but is also fed via the 1436 keV γ-ray decay from the 2321 keV state. Therefore, the population cross section for the 2_1^+ state is the difference between the production cross sections for the 885 and 1436 keV γ-rays. We are not aware about the spin and parity assigments of the 2321 keV state; however, we can limit the possible J^π values for this state by requiring that the reduced matrix elements $B(\lambda; 0^+_{gs} \rightarrow \lambda^\pi)$ corresponding to the observed experimental yield for the 2321 keV state are consistent with the recommended upper limits listed by Endt [13]. This condition gives the possible J^π values for the 2321 keV state as 1^- (for which the measured cross section would give $B(E1; 0^+_{gs} \rightarrow 1^-) = 0.040(16)\ e^2fm^2$) or 2^+ (which gives $B(E2; 0^+_{gs} \rightarrow 2^+) = 105(42)\ e^2fm^4$). When this is subtracted from the γ-ray production cross section for the 885 keV γ-ray, we obtain $B(E2; 0^+_{gs} \rightarrow 2_1^+) = 333(70)\ e^2fm^4$ for ^{32}Mg.

Motobayashi [7] did not report the observation of the 1436 keV γ-ray. However, it is worth noting that the difference between the $B(E2; 0^+_{gs} \rightarrow 2_1^+)$ values obtained in Ref. [7] and the present work can be accounted for by the feeding correction applied here. Without the feeding correction, we would obtain $B(E2; 0^+_{gs} \rightarrow 2_1^+) = 440(55)\ e^2fm^4$, which would be consistent with the result from Ref. [7] of $B(E2; 0^+_{gs} \rightarrow 2_1^+) = 454(78)\ e^2fm^4$.

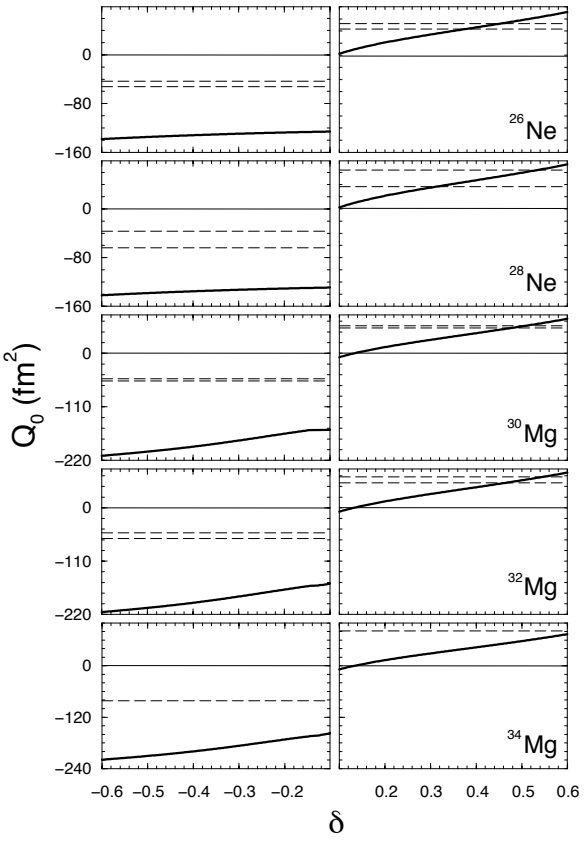

Figure 2: Calculations of electric quadrupole moments as a function of the deformation parameter δ for ^{26,28}Ne and ^{30,32,34}Mg. The "experimental" electric quadrupole moments are shown as bands bounded by dashed lines corresponding to experimental uncertainties. The bands are located at both positive and negative values since the present data do not distinguish between prolate and oblate deformations.

The secondary ^{34}Mg beam was particularly weak, and the integrated number of beam particles was small. However, we can still draw some conclusions from the γ-ray spectrum. The data are not sufficient to identify the energy of the 2_1^+ state. Assuming that 2_1^+ state is located between 0.9 and 1.4 MeV, we can place an upper limit on $B(E2; 0_{gs}^+ \rightarrow 2_1^+)$ of 670 e^2fm^4.

While the spherical shell model has been used extensively to study the nuclei in the vicinity of the island of inversion [14], the deformed shell model, or Nilsson model, provides another framework for gaining insights about isotopes in this region. If we assume that the nuclei studied here have static quadrupole deformations with axial symmetry, we can use the Nilsson model [15] to calculate intrinsic quadrupole moments for oblate and prolate shapes. With this Nilsson diagram, the intrinsic electric quadrupole moments Q_0 have been calculated for the nuclei studied here over a range of deformations by summing over the contributions of the individual protons

$$Q_0 = (16\pi/5)^{1/2}\Sigma_\lambda \langle\lambda|r^2 Y_{20}|\lambda\rangle, \quad (1)$$

where λ are the occupied proton orbitals. The intrinsic quadrupole moments are graphed as a function of δ for ^{26,28}Ne and ^{30,32,34}Mg in Fig. 2. The figures do not include quadrupole moment results for the range of small δ values ($-0.1 < \delta < 0.1$) where residual interaction outside of the standard Nilsson model becomes important. The deformation parameter used in the diagram is δ, which is related to the usual spherical

harmonic coefficient β_{20} (or just β_2) by $\beta_2 = \delta/0.95$. This figure also illustrates the "experimental" intrinsic electric quadrupole moments extracted from the measured $B(E2; 0^+_{gs} \rightarrow 2^+_1)$ [16]. The bands shown in Fig. 2 as dashed lines correspond to the ranges of experimental uncertainty in the present work. Both positive and negative experimental values are shown in the graphs because our experiment cannot discriminate between prolate and oblate shapes. For all the nuclei in Fig. 2, it is clear that the "experimental" quadrupole moments can be reproduced if the nuclei have substantial prolate deformations ($\delta \geq 0.3$).

In conclusion, we have measured $E(2^+_1)$ and $B(E2; 0^+_{gs} \rightarrow 2^+_1)$ in ^{26,28}Ne and ^{30,32}Mg. In addition, we have placed an upper limit on $B(E2; 0^+_{gs} \rightarrow 2^+_1)$ in ^{34}Mg. We find that the energies and $B(E2; 0^+_{gs} \rightarrow 2^+)$ values for the lowest 2^+ states in the $N = 16$ isotope ^{26}Ne and the $N = 18$ isotope ^{30}Mg can be explained using the normal $0\hbar\omega$ configurations, while the energy of the 2^+_1 state in ^{28}Ne suggests strong mixing between the intruder and normal configurations in this nucleus. We find that $B(E2; 0^+_{gs} \rightarrow 2^+)$ value for the lowest 2^+ state in ^{32}Mg to be 27% lower than the value reported by Motobayashi *et al.* [7]. We also present deformed shell model calculations which demonstrate that if these nuclei have static axially symmetric deformations, they must be prolate.

This work was supported by the National Science Foundation through grant numbers PHY-9523974, PHY-9528844, and PHY-9605207.

a. Department of Physics, Florida State University, Tallahassee, FL 32306, USA

References

1. C. Thibault *et al.*, Phys. Rev. C12 (1975) 644.
2. W. Chung and B.H. Wildenthal, Phys. Rev. C22 (1980) 2260.
3. C. Detraz *et al.*, Nucl. Phys. A394 (1983) 378.
4. D.J. Viera *et al.*, Phys. Rev. Lett. 57 (1986) 3253.
5. E.K. Warburton, J.A. Becker and B.A. Brown, Phys. Rev. C41 (1990) 1147.
6. C. Detraz *et al.*, Phys. Rev. C19 (1979) 164.
7. T. Motobayashi *et al.*, Phys. Lett. B 346 (1995) 9.
8. B. M. Sherill *et al.*, Nucl. Instr. Meth. B 56 (1991) 1106.
9. M.J. Lopez-Jimenez *et al.*, contribution to XXXVII International Winter meeting on Nuclear Physics (Bormio, Italy, January 1999).
10. D. Guillemaud-Mueller *et al.*, Nucl. Phys. A426 (1984) 37.
11. G. Klotz *et al.*, Phys. Rev. C47 (1993) 2502.
12. A. Winther and K. Adler, Nucl. Phys. A319 (1979) 518.
13. P.M. Endt, At. Data Nucl. Data Tables 55 (1993) 171.
14. E. Caurier *al.*, Phys. Rev. C58 (1998) 2033.
15. S.G. Nilsson and I. Ragnarsson, Shapes and Shells in Nuclear Structure (Cambridge University Press, Cambridge, 1995).
16. A. Bohr and B.R. Mottelson, Nuclear Structure, Vol.2, (World Scientific, 1998).